

# Safety Alignment as Continual Learning: Mitigating the Alignment Tax via Orthogonal Gradient Projection

Guanglong Sun <sup>\*1,2</sup> Siyuan Zhang <sup>\*3</sup> Liyuan Wang <sup>4</sup> Jun Zhu <sup>3</sup> Hang Su <sup>3</sup> Yi Zhong <sup>1,2</sup>

## Abstract

Large Language Models (LLMs) often incur an *alignment tax*: safety post-training can reduce general utility (e.g., reasoning and coding). We argue that this tax primarily arises from continual-learning-style forgetting in sequential alignment, where distribution shift and conflicting objectives cause safety updates to overwrite pre-trained competencies. Accordingly, we cast safety alignment as a **continual learning (CL)** problem that must balance **plasticity** (acquiring safety constraints) and **stability** (preserving general abilities). We propose **Orthogonal Gradient Projection for Safety Alignment (OGPSA)**, a lightweight method that mitigates interference by constraining each safety update to be orthogonal (in a first-order sense) to a learned subspace capturing general capabilities. Specifically, OGPSA estimates a low-rank capability subspace from gradients on a small reference set and projects the safety gradient onto its orthogonal complement before updating. This produces safety-directed updates that minimally perturb prior knowledge while retaining capacity for alignment. OGPSA is plug-and-play and integrates into standard post-training pipelines without large-scale replay, auxiliary objectives, or retraining. Across *Supervised Fine-Tuning (SFT)*, *Direct Preference Optimization (DPO)*, and sequential *SFT*→*DPO* settings, OGPSA consistently improves the safety–utility Pareto frontier over standard baselines. For instance, on Qwen2.5-7B-Instruct under *SFT*→*DPO*, OGPSA preserves

strong safety while recovering general capability, improving *SimpleQA* from 0.53% to 3.03% and *IFEval* from 51.94% to 63.96%. Our source code is available at [OGPSA](#)

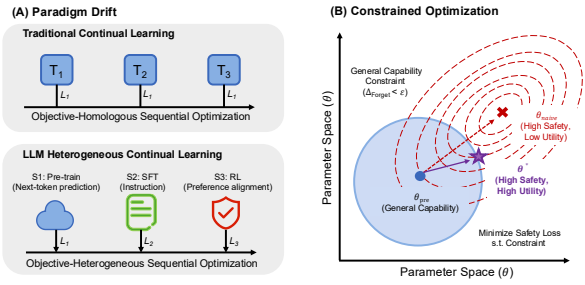


Figure 1. Conceptual framework for reframing LLM Safety Alignment as a Constrained Continual Learning Problem. (A) Comparison of traditional CL and LLM Heterogeneous CL. (B) Safety alignment under anti-forgetting constraints.

## 1. Introduction

Large Language Models (LLMs) have emerged as highly capable general-purpose systems (Achiam et al., 2023; Bai et al., 2023; Dubey et al., 2024), achieving strong performance in complex reasoning (Cobbe et al., 2021; Hendrycks et al., 2021b), code generation (Chen et al., 2021; Nam et al., 2024), and open-ended content synthesis (Sudhakaran et al., 2023; Kantharaj et al., 2022; Liu et al., 2025). However, capability alone does not imply safe or aligned behavior: without explicit alignment, LLMs may generate toxic or biased outputs, produce persuasive misinformation, or provide assistance that enables harmful actions (Dong et al., 2023; Liu et al., 2023; Wang et al., 2023). As a result, safety and reliability have become central requirements for deployment, often summarized by the desiderata of being **helpful, honest, and harmless (HHH)** (Ouyang et al., 2022).

In practice, safety alignment is typically implemented via a dedicated *post-training* pipeline (Wang et al., 2024c). After large-scale pre-training endows broad general capabilities, the model is further optimized to follow human intent and safety constraints using *Supervised Fine-Tuning (SFT)* (Bianchi et al., 2024; Choi et al., 2024) and/or preference-based optimization such as *RLHF* (Ouyang et al.,

<sup>1</sup>School of Life Sciences, IDG/McGovern Institute for Brain Research, Tsinghua University, Beijing, China <sup>2</sup>Tsinghua–Peking Joint Center for Life Sciences <sup>3</sup>Dept. of Comp. Sci. and Tech., Institute for AI, Tsinghua-Bosch Joint ML Center, THBI Lab, BNRist Center, Tsinghua University, Beijing, China <sup>4</sup>Department of Psychological and Cognitive Sciences, Tsinghua University, Beijing, China. Correspondence to: Hang Su <[suhangss@mail.tsinghua.edu.cn](mailto:suhangss@mail.tsinghua.edu.cn)>, Yi Zhong <[zhongyithu@tsinghua.edu.cn](mailto:zhongyithu@tsinghua.edu.cn)>.

2022; Dai et al., 2024) or *Direct Preference Optimization (DPO)* (Rafailov et al., 2023). While effective at reducing harmful behaviors, this sequential optimization frequently incurs an **alignment tax**: improving safety can lead to measurable regressions in general capabilities (e.g., truthfulness or general helpfulness, see naive tuning in Fig. 2) (Ouyang et al., 2022; Askell et al., 2021; Noukhovitch et al., 2023). A key driver is *parameter interference across different stages*—updates induced by safety objectives can modify the same parameter subspaces that encode pre-trained competencies, yielding capability loss even as safety improves (Kirk et al., 2024; Lin et al., 2024).

Recent work attempts to mitigate this trade-off by *anchoring* post-training updates to the pre-trained model through two common mechanisms. First, *rehearsal/replay* interleaves a subset of general data or auxiliary pre-training-style objectives during alignment (e.g., PPO-PTX in Instruct-GPT (Ouyang et al., 2022)), which can reduce regressions but increases compute and introduces additional scheduling and mixture hyperparameters (Lin et al., 2024). Second, *proximity regularization* constrains the aligned policy to remain close to a reference model, most prominently via KL penalties in PPO-style RLHF and related preference-optimization objectives (Papineni et al., 2002; Yang et al., 2024a; Huang et al., 2021). Although these techniques often improve capability retention, these approaches introduce significant burdens, including elevated data requirements, architectural complexity, and dependency on sensitive hyperparameters like the replay ratio or KL penalty (Zhang et al., 2025; Lin et al., 2024). More fundamentally, they act as *soft constraints*: they shrink the overall update or penalize distributional deviation, but do not explicitly remove the components of the safety update that interfere with capability-preserving directions in parameter space. Consequently, safety gradients may still project onto subspaces that encode pre-trained competencies, leading to (*catastrophic*) *forgetting*—a measurable drop in performance on previously acquired general skills after alignment.

To move beyond such heuristic anchoring, we interpret the alignment tax as a principled instance of catastrophic forgetting under *objective-heterogeneous* sequential optimization (Fig. 1A). This yields a key observation specific to modern LLM alignment: post-training is inherently a **Continual Learning (CL)** process, where the model is updated across multiple training stages (e.g., SFT followed by preference optimization) that induce heterogeneous shifts in *both* data distributions and optimization objectives (Ouyang et al., 2022; Lin et al., 2024). From the perspective of CL, the alignment tax arises because safety-induced gradients inadvertently overwrite parameter subspaces critical for general capabilities. This fundamental conflict mirrors the classic *stability–plasticity dilemma* (Wang et al., 2024a; Zhou et al., 2024a): effective alignment demands the *plasticity* to

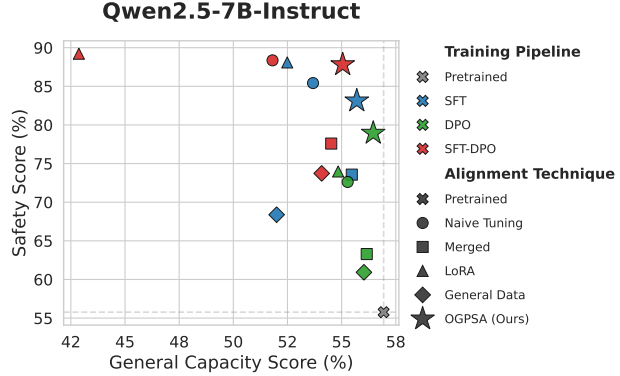


**Figure 2. Overall performance of alignment strategies on Qwen2.5-7B-Instruct.** We report the aggregate *Safety Score* (avg. of 4 datasets) and *General Capacity Score* (avg. of 6 datasets); see Table 1 for details and Appendix Figure 4 for the Llama3.1-8B-Instruct results.

acquire new safety constraints without compromising the *stability* of pre-trained general knowledge (Fig. 1B). Accordingly, the core challenge is not merely to regularize the update magnitude, but to design updates that satisfy safety objectives *while explicitly minimizing interference* with the parameter subspaces that support general capabilities.

To bridge this gap, we introduce a unified optimization framework that addresses the root cause of the alignment tax: *directional interference* between safety-driven updates and capability-preserving parameter subspaces. We propose **Orthogonal Gradient Projection for Safety Alignment (OGPSA**, Fig. 3), a lightweight geometric procedure that utilizes an explicit constraint, rather than heuristic anchoring, to decouple safety acquisition from capability retention. OGPSA employs a small, representative subset of general data to identify a low-dimensional gradient subspace essential for stabilizing core competencies. During alignment (e.g., via SFT or DPO), the method projects safety gradients onto the orthogonal complement of this capability subspace. This effectively filters out update components that risk overwriting capability-critical directions. Consequently, OGPSA facilitates robust safety improvements without the need for massive data replay, heavy regularization, or costly re-training, and can be integrated into standard post-training pipelines in a plug-and-play manner. Extensive experiments across multiple benchmarks show that OGPSA significantly mitigates alignment tax (Fig. 2, Table 1). This leads to a more favorable safety–capability trade-off than standard baselines, yielding a distinctly superior Pareto frontier.

Our main contributions are summarized as follows:

- We reframe safety alignment as a continual learning problem, characterizing the “alignment tax” as a form of catastrophic forgetting driven by the stability–plasticity dilemma where sequential, heterogeneous optimization erodes pre-trained capabilities.

- We propose OGSPA, a lightweight, plug-and-play gradient projection algorithm, projecting the safety gradient onto the orthogonal space of general capabilities thereby decoupling safety optimization from capability forgetting.
- We conduct extensive experiments across various model families and alignment strategies, demonstrating that OGSPA serves as a robust solution for mitigating the alignment tax, achieving a superior Pareto frontier between safety and general abilities compared to standard baselines.

## 2. Related Work

**LLM Safety Alignment.** Research on safety alignment for LLMs primarily centers on two perspectives. The first line of work involves *test-time intervention*, which introduces external safety guards to identify unsafe responses (Inan et al., 2023; Lee et al., 2025; Jaech et al., 2024; Wang et al., 2024d) or actively adjusts the output distribution via model steering (Kowsher et al., 2025; Rebedea et al., 2025; Wu et al., 2025a). However, these approaches invariably incur additional inference latency and increase system complexity. The second perspective focuses on *post-training* the model for safety awareness. Nevertheless, simply training the model on safety data often leads to a degradation in general capabilities (Ouyang et al., 2022; Askell et al., 2021; Noukhovitch et al., 2023). Existing methods attempt to mitigate this by introducing replay data to preserve original abilities or designing task-specific pipelines (Ouyang et al., 2022; Lin et al., 2024; Zhang et al., 2025). Yet, the former solution significantly increases training computational costs, while the latter complicates the training pipeline and lacks universality across different training pipeline (Wang et al., 2024c). Moreover, both solutions are largely heuristic, lacking theoretical guarantees for the training outcomes (Lin et al., 2024). In contrast, our method, derived from a rigorous continual learning framework, provides a theoretical guarantee for both safety enhancement and the preservation of general capabilities. Furthermore, its ease of implementation renders our method applicable to diverse training processes with negligible additional cost.

**Continual Learning.** Continual Learning (CL) aims to enable models to learn sequential tasks without suffering from catastrophic forgetting, addressing the classic stability-plasticity dilemma (Wang et al., 2024a; Zhou et al., 2024a). Traditional CL methods generally fall into three categories: (1) *Regularization-based methods* which impose penalty terms on important parameters to restrict their changes (e.g., EWC (Kirkpatrick et al., 2017), LwF (Li & Hoiem, 2017)) ; (2) *Replay-based methods* which retain a buffer of historical data for rehearsal (e.g., GEM (Lopez-Paz & Ranzato, 2017), DER (Buzzeaga et al., 2020)); and (3) *Optimization-based*

*methods* which decouple parameter updates at the gradient level to facilitate the learning of new tasks while effectively preserving pre-existing knowledge (Lu et al., 2024; Qiao et al., 2025; Lin et al., 2022). More recently, advanced CL methods have shifted toward leveraging pretrained models via parameter-efficient tuning (Wang et al., 2022; Wu et al., 2025b) and representation alignment (Zhang et al., 2023; McDonnell et al., 2024) to achieve superior rehearsal-free performance. Since safety alignment parallels CL in the fundamental goal of mitigating catastrophic forgetting, it can directly leverage the latter’s established theoretical framework. However, while effective in standard settings, most existing CL research assumes a sequence of tasks with a *homogeneous* optimization objective (e.g., a sequence of classification tasks) where only the data distribution shifts. In contrast, the LLM training lifecycle involves a *multi-stage* process where both the data distribution and the optimization objective shift drastically (Ouyang et al., 2022; Lin et al., 2024). Consequently, the direct application of traditional methods presents challenges due to the *objective heterogeneity* (i.e., shifting loss landscapes from likelihood to ranking), underscoring the need for a tailored approach to explicitly reconcile the optimization conflicts between safety acquisition and capability preservation.

## 3. Preliminaries

We study *sequential post-training* for safety alignment and its tendency to reduce general utility (the *alignment tax*). We first formalize the tax as capability forgetting induced by distribution or objective shifts, and then derive a tractable *first-order* constraint that directly motivates our method.

### 3.1. Sequential Safety Alignment and the Alignment Tax

Let  $\theta_{\text{pre}}$  denote the parameters of a pre-trained LLM trained on a broad next-token objective. Safety alignment then applies one or more post-training stages (e.g., SFT, DPO (Rafailov et al., 2023)), producing  $\theta_{\text{safe}}$ . While these stages improve safety behavior, they can degrade general utility.

Let  $\Phi(\theta; \mathcal{D}_{\text{eval}})$  be an evaluation metric on a general evaluation suite  $\mathcal{D}_{\text{eval}}$ . We define the alignment tax as

$$\Delta_{\text{tax}} = \Phi(\theta_{\text{pre}}; \mathcal{D}_{\text{eval}}) - \Phi(\theta_{\text{safe}}; \mathcal{D}_{\text{eval}}). \quad (1)$$

In practice, directly constraining  $\Phi$  during training is difficult (often non-differentiable or expensive) so we introduce a differentiable *capability surrogate*.

### 3.2. Heterogeneous Continual Learning Perspective

Safety alignment is naturally modeled as *heterogeneous continual learning* (HCL) because the post-training pipeline is *sequential* and each stage typically changes both the *data*

distribution and the objective (Fig. 1A) (Ouyang et al., 2022; Lin et al., 2024). Starting from a pre-trained model  $\theta_{\text{pre}}$  learned on a broad pre-training distribution, alignment proceeds through stages such as instruction tuning and preference optimization, e.g., SFT and DPO on safety dataset  $\mathcal{D}_{\text{safe}}$ . Importantly, these stages do not merely introduce new samples; they also alter the risk functional (likelihood-based supervision  $\rightarrow$  preference/ranking-based optimization, which can substantially reshape gradient geometry.

Consider a generic alignment stage that optimizes a safety-related objective  $\mathcal{L}_{\text{safe}}(\theta)$  (e.g., SFT or the DPO (Rafailov et al., 2023) loss). A standard gradient update takes the form

$$\theta \leftarrow \theta - \eta g_{\text{safe}}, \quad g_{\text{safe}} := \nabla_{\theta} \mathcal{L}_{\text{safe}}(\theta), \quad (2)$$

where  $\eta$  is learning rate. Under HCL, the alignment tax can be interpreted as continual-learning-style forgetting: due to distribution shift and objective shift across stages,  $g_{\text{safe}}$  may contain significant components along parameter directions that encode general capabilities acquired during pre-training. Consequently, the naive update in Eq. (2) can overwrite capability-supporting parameters while improving safety behavior, yielding a degradation in general utility (Fig. 1B).

### 3.3. First-Order Capability Preservation via Gradient Orthogonality

Leveraging the insight that the parameter space governing general capabilities exhibits low intrinsic dimensionality (Aghajanyan et al., 2021; Zhou et al., 2023a), we counter heterogeneous continual learning style forgetting by estimating the gradient subspace critical for preserving core capabilities with a small *reference* collection of general-purpose data. Let  $\{\mathcal{D}_{\text{ref}}^{(i)}\}_{i=1}^M$  be  $M$  small datasets, each targeting a facet of general ability (e.g., reasoning, coding, truthfulness). Let  $\mathcal{L}_{\text{ref}}^{(i)}(\theta)$  denote a differentiable loss on  $\mathcal{D}_{\text{ref}}^{(i)}$  (e.g., cross-entropy), and define the corresponding reference gradients

$$g^{(i)}(\theta) := \nabla_{\theta} \mathcal{L}_{\text{ref}}^{(i)}(\theta), \quad i = 1, \dots, M. \quad (3)$$

Consider a small parameter update  $\Delta\theta$ . A first-order Taylor expansion gives

$$\mathcal{L}_{\text{ref}}^{(i)}(\theta + \Delta\theta) \approx \mathcal{L}_{\text{ref}}^{(i)}(\theta) + \langle g^{(i)}(\theta), \Delta\theta \rangle. \quad (4)$$

Thus, a sufficient condition to preserve reference capability  $i$  to first order is  $\langle g^{(i)}(\theta), \Delta\theta \rangle = 0$ . Enforcing this for all  $i$  yields the linear constraints

$$\langle g^{(i)}(\theta), \Delta\theta \rangle = 0, \quad i = 1, \dots, M. \quad (5)$$

We summarize these directions via the *general-capability subspace*

$$\mathcal{S}_{\text{gen}}(\theta) := \text{span}\{g^{(1)}(\theta), \dots, g^{(M)}(\theta)\}. \quad (6)$$

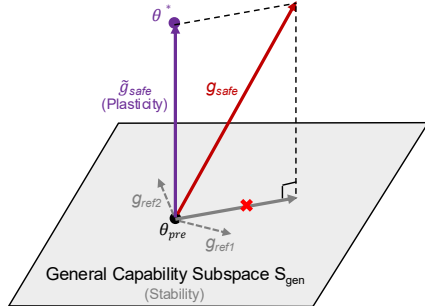


Figure 3. Schematic illustration of the proposed Orthogonal Gradient Projection for Safety Alignment (OGPSA) framework.  $g_{\text{ref}1}, g_{\text{ref}2}$ : Reference gradients computed from representative general capability datasets (e.g., helpfulness, truthfulness).  $g_{\text{safe}}$ : The standard gradient derived from the safety alignment objective.  $\tilde{g}_{\text{safe}}$ : The projected safety gradient obtained by projecting  $g_{\text{safe}}$  onto the orthogonal space of the general capability subspace.

Equation (5) is equivalent to requiring  $\Delta\theta \in \mathcal{S}_{\text{gen}}(\theta)^\perp$ . This yields the first-order remedy behind our method: *perform safety optimization only along directions orthogonal to the local general-capability subspace*. The next section operationalizes this principle by maintaining a low-rank basis for  $\mathcal{S}_{\text{gen}}(\theta)$  and projecting each safety gradient accordingly, resulting in an efficient plug-and-play update rule.

## 4. Methodology

In this section, we present **Orthogonal Gradient Projection for Safety Alignment (OGPSA**, Fig. 3), a plug-and-play update rule that mitigates the *alignment tax* by reducing *gradient interference* between safety optimization and pre-trained general capabilities. OGPSA estimates a low-rank general-capability subspace from reference gradients and projects each safety gradient onto its orthogonal complement before updating parameters.

### 4.1. Overview

Modern alignment is typically performed *sequentially* after pre-training, and often across multiple stages with shifting objectives and data distributions (e.g., likelihood-based SFT on  $\mathcal{D}_{\text{sft}}$  followed by preference optimization on  $\mathcal{D}_{\text{safe}}$ ). This setting is naturally viewed as *heterogeneous continual learning*, where both the task objective and the training distribution change over time. Consequently, a naive safety update through Eq. 2 can overwrite parameter directions that are important for broad utility, inducing continual-learning-style forgetting.

OGPSA constrains each safety step to avoid directions that locally encode general capability. Concretely, we maintain a low-rank *general-capability subspace*  $\mathcal{S}_{\text{gen}}(\theta)$  estimated from reference gradients  $\{g^{(i)}(\theta)\}_{i=1}^M$  computed on small, diverse general-capability datasets. We then update parameters using only the component of the safety gradient

orthogonal to this subspace:

$$\Delta\theta = -\eta P_{\mathcal{S}_{\text{gen}}(\theta)^\perp}(g_{\text{safe}}(\theta)), \quad \theta \leftarrow \theta + \Delta\theta. \quad (7)$$

Equivalently, letting  $U$  denote an orthonormal basis of  $\mathcal{S}_{\text{gen}}(\theta)$  (rank  $M'$ ), the projected direction is  $\tilde{g}_{\text{safe}} = g_{\text{safe}} - U(U^\top g_{\text{safe}})$ , and we take  $\theta \leftarrow \theta - \eta \tilde{g}_{\text{safe}}$ .

The subspace is refreshed periodically (every  $K$  steps) using inexpensive reference mini-batches, and the projection requires only a small number of inner products for low rank  $M'$ . As a result, OGSPA is lightweight and directly applicable across alignment stages (e.g., SFT/DPO/RLHF-style updates) without modifying the underlying training pipeline.

We next describe dynamic subspace construction, the projected update rule with its first-order justification, and the resulting algorithm and computational overhead (see Fig. 3 and Algorithm 1).

## 4.2. General-Capability Subspace Estimation

Directly constraining general-utility metrics during training is typically infeasible. Instead, we approximate capability preservation using a small set of differentiable *reference* objectives (Aghajanyan et al., 2021; Zhou et al., 2023a). Let  $\{\mathcal{D}_{\text{ref}}^{(i)}\}_{i=1}^M$  be  $M$  small datasets, each targeting one facet of general capability (e.g., reasoning, coding, truthfulness). For each dataset, we define a differentiable loss  $\mathcal{L}_{\text{ref}}^{(i)}(\theta)$  (e.g., cross-entropy) and its gradient

$$g^{(i)}(\theta) := \nabla_\theta \mathcal{L}_{\text{ref}}^{(i)}(\theta), \quad i = 1, \dots, M. \quad (8)$$

We define the *general-capability subspace* as the span of these gradients:

$$\mathcal{S}_{\text{gen}}(\theta) := \text{span}\{g^{(1)}(\theta), \dots, g^{(M)}(\theta)\}. \quad (9)$$

**Dynamic, low-rank basis.** Since the local geometry can shift as training progresses, we update the subspace periodically. Every  $K$  steps (i.e., at step  $\tau$ ), we compute  $M$  reference gradients on mini-batches  $B^{(i)} \sim \mathcal{D}_{\text{ref}}^{(i)}$  and construct an orthonormal basis  $U_\tau = [u_{\tau,1}, \dots, u_{\tau,M'}] \in \mathbb{R}^{d \times M'}$  for  $\mathcal{S}_{\text{gen}}(\theta_\tau)$ .  $M'$  denotes the rank of the estimated subspace, where  $M' \leq M$  accounts for the potential removal of linearly dependent directions. We employ the Gram–Schmidt process (Björck, 1994; Leon et al., 2013) with a threshold  $\delta$  to filter out redundancy:

$$u_{\tau,1} = \frac{g_\tau^{(1)}}{\|g_\tau^{(1)}\| + \epsilon}, \quad (10)$$

$$\begin{aligned} v_{\tau,k} &= g_\tau^{(k)} - \sum_{j=1}^{k-1} \langle g_\tau^{(k)}, u_{\tau,j} \rangle u_{\tau,j}, \\ u_{\tau,k} &= \frac{v_{\tau,k}}{\|v_{\tau,k}\| + \epsilon} \quad \text{if } \|v_{\tau,k}\| \geq \delta, \end{aligned} \quad (11)$$

discarding nearly collinear directions when  $\|v_{\tau,k}\| < \delta$ .

## Algorithm 1 OGSPA: Orthogonal Gradient Projection for Safety Alignment

---

**Require:** Pre-trained parameters  $\theta_0$ , safety loss  $\mathcal{L}_{\text{safe}}$ , reference datasets  $\{\mathcal{D}_{\text{ref}}^{(i)}\}_{i=1}^M$ , refresh period  $K$ , learning rate  $\eta$ .

**Ensure:** Aligned parameters  $\theta_T$ .

- 1: Initialize  $U \leftarrow []$
- 2: **for**  $t = 0, \dots, T-1$  **do**
- 3:     **{Dynamic Subspace Construction (refresh every  $K$  steps)}**
- 4:     **if**  $t \bmod K = 0$  **then**
- 5:         **for**  $i = 1$  to  $M$  **do**
- 6:             Sample  $B^{(i)} \sim \mathcal{D}_{\text{ref}}^{(i)}$
- 7:             Compute  $g^{(i)} \leftarrow \nabla_\theta \mathbb{E}_{\xi \in B^{(i)}} [\ell_{\text{ref}}^{(i)}(\theta_t; \xi)]$
- 8:         **end for**
- 9:         Construct orthonormal basis  $U \leftarrow \text{GramSchmidt}(\{g^{(i)}\}_{i=1}^M)$   $\triangleright U \equiv U_\tau$
- 10:     **end if**
- 11:     **{Projected Safety Optimization}**
- 12:     Compute safety gradient  $g_{\text{safe}} \leftarrow \nabla_\theta \mathcal{L}_{\text{safe}}(\theta_t)$
- 13:     Project  $\tilde{g}_{\text{safe}} \leftarrow g_{\text{safe}} - U(U^\top g_{\text{safe}})$   $\triangleright$  Remove conflicting components
- 14:     Update  $\theta_{t+1} \leftarrow \theta_t - \eta \tilde{g}_{\text{safe}}$
- 15:     **end for**
- 16: **Return**  $\theta_T$

---

## 4.3. Projected Safety Optimization

At training iteration  $t$ , let  $g_{\text{safe}} := \nabla_\theta \mathcal{L}_{\text{safe}}(\theta_t)$  denote the safety gradient. OGSPA maintains a (lagged) orthonormal basis  $U_\tau = [u_{\tau,1}, \dots, u_{\tau,M'}] \in \mathbb{R}^{d \times M'}$  for the current general-capability subspace  $\mathcal{S}_{\text{gen}}(\theta) \approx \text{span}\{g^{(i)}(\theta)\}_{i=1}^M$ , refreshed every  $K$  steps (so  $\tau = \lfloor t/K \rfloor$ ). We remove the components of  $g_{\text{safe}}$  that lie in  $\mathcal{S}_{\text{gen}}(\theta)$  by projecting onto its orthogonal complement:

$$\tilde{g}_{\text{safe}} = g_{\text{safe}} - U_\tau(U_\tau^\top g_{\text{safe}}) = g_{\text{safe}} - \sum_{j=1}^{M'} \langle g_{\text{safe}}, u_{\tau,j} \rangle u_{\tau,j}. \quad (12)$$

We then perform the projected update

$$\theta_{t+1} \leftarrow \theta_t - \eta \tilde{g}_{\text{safe}}. \quad (13)$$

Intuitively, (12)–(13) enforce that each safety step lies in  $\mathcal{S}_{\text{gen}}(\theta)^\perp$  (up to the refresh lag), thereby reducing first-order interference with general-capability directions.

**First-order preservation and optimality.** We justify the projection rule via a first-order preservation argument. Consider a local parameter perturbation  $\Delta\theta$ . For each reference objective, a first-order expansion yields

$$\mathcal{L}_{\text{ref}}^{(i)}(\theta + \Delta\theta) \approx \mathcal{L}_{\text{ref}}^{(i)}(\theta) + \langle g^{(i)}(\theta), \Delta\theta \rangle. \quad (14)$$

**Table 1. Comparative evaluation of safety alignment and general capability retention.** We compare our method (OGPSA) against standard baselines (SFT, DPO (Rafailov et al., 2023), SFT-DPO) and mitigation strategies (Merge, LoRA, Data Mixing) across Llama3.1-8B-Instruct and Qwen2.5-7B-Instruct Model. Our method achieves a Pareto-superior trade-off, significantly mitigating the alignment tax. The **best** and second-best results are marked in **bold** and underlined, respectively.

Model	Safety ( $\uparrow$ )				Truthful ( $\uparrow$ )			Helpful ( $\uparrow$ )		Robustness ( $\uparrow$ )
	XSTest	WildChat	Stereotype	StrongReject	SimpleQA	GPQA	MMLU	IFEval	HHH	AdvGLUE
<b>Llama3.1-8B-Instruct Model</b>										
Instruct Baseline	88.50	15.80	89.85	56.59	1.90	22.90	71.07	67.28	86.61	46.30
<b>SFT</b>	83.00	<b>50.00</b>	89.08	<b>97.27</b>	0.72	24.58	70.00	57.12	87.89	41.92
+ Merge	79.00	31.20	<u>92.02</u>	77.34	1.43	23.91	<u>70.64</u>	<b>63.96</b>	<u>87.48</u>	<b>44.92</b>
+ LoRA	<u>85.99</u>	42.60	85.63	<b>96.62</b>	0.42	<u>24.92</u>	69.07	51.20	87.48	40.73
+ General Data	85.50	14.40	89.46	71.38	<u>3.54</u>	23.40	67.43	58.60	83.74	42.52
+ OGPSA (Ours)	<b>86.00</b>	47.00	<b>92.53</b>	94.81	<u>2.88</u>	<b>25.59</b>	<b>70.93</b>	<u>60.26</u>	<b>89.18</b>	<u>43.59</u>
<b>DPO</b>	81.00	<u>42.80</u>	70.31	<b>97.66</b>	0.25	23.57	66.21	41.22	77.92	33.17
+ Merged	<u>88.00</u>	30.80	<u>88.89</u>	73.22	1.27	<b>25.42</b>	70.36	63.36	84.97	45.40
+ LoRA	82.50	<b>43.80</b>	72.41	<u>87.35</u>	0.62	21.72	69.64	58.99	<u>85.36</u>	43.05
+ General Data	63.00	15.40	<b>90.42</b>	57.28	<u>2.59</u>	<u>24.24</u>	<u>71.36</u>	<b>64.51</b>	<b>87.09</b>	<b>50.30</b>
+ OGPSA (Ours)	<b>95.00</b>	38.40	75.86	85.89	<b>3.05</b>	23.57	<b>71.57</b>	<u>63.77</u>	83.71	<u>49.59</u>
<b>SFT-DPO</b>	87.00	<u>59.40</u>	72.61	<u>99.87</u>	0.28	26.94	69.00	43.25	84.53	34.51
+ Merged	82.00	36.00	<u>89.46</u>	83.29	1.04	24.92	<b>70.21</b>	<b>62.11</b>	<b>87.44</b>	43.67
+ LoRA	81.50	<b>80.80</b>	58.05	<b>99.93</b>	0.07	10.27	61.21	16.82	82.04	26.29
+ General Data	<u>89.00</u>	17.60	<b>94.44</b>	75.73	<b>4.05</b>	<b>29.46</b>	66.71	<u>59.15</u>	84.15	<b>44.71</b>
+ OGPSA (Ours)	<b>91.50</b>	45.80	88.12	94.48	<u>3.28</u>	<u>27.95</u>	70.00	57.67	<u>84.98</u>	<u>43.73</u>
<b>Qwen2.5-7B-Instruct Model</b>										
Instruct Baseline	65.50	16.00	96.74	44.83	3.33	34.18	73.50	64.33	88.77	77.55
<b>SFT</b>	87.00	<u>64.20</u>	<b>100.00</b>	<u>90.48</u>	0.79	<u>34.18</u>	72.00	57.30	88.34	69.48
+ Merged	83.00	45.60	99.04	66.65	2.24	34.04	<u>72.64</u>	<u>61.74</u>	88.34	<u>73.82</u>
+ LoRA	<u>88.00</u>	<b>68.80</b>	<b>100.00</b>	<b>95.54</b>	0.67	32.83	71.50	51.39	<u>88.77</u>	69.78
+ General Data	77.50	26.60	99.04	70.38	<u>3.47</u>	23.57	69.93	53.42	86.28	<b>75.35</b>
+ OGPSA (Ours)	<u>87.50</u>	57.60	<b>100.00</b>	87.37	<b>3.61</b>	<b>34.68</b>	<b>73.21</b>	<b>63.03</b>	<b>89.97</b>	69.72
<b>DPO</b>	<u>87.00</u>	41.40	98.47	63.60	1.57	31.31	<u>73.43</u>	<u>63.22</u>	87.52	74.60
+ Merged	79.50	26.20	97.32	50.12	2.59	31.99	<b>74.00</b>	62.48	<u>89.62</u>	<u>76.25</u>
+ LoRA	85.50	<u>42.80</u>	<u>98.66</u>	<u>68.96</u>	0.97	31.14	73.36	61.55	89.21	72.80
+ General Data	78.50	21.00	97.32	46.89	<u>3.29</u>	<u>32.15</u>	73.21	62.85	87.92	<b>76.73</b>
+ OGPSA (Ours)	<b>94.50</b>	<b>49.40</b>	<b>99.23</b>	<b>72.64</b>	<b>3.35</b>	<b>34.51</b>	72.79	<b>63.40</b>	<b>90.68</b>	74.05
<b>SFT-DPO</b>	<b>92.50</b>	<u>65.80</u>	<u>99.62</u>	95.53	0.53	30.98	<u>72.14</u>	51.94	88.36	66.92
+ Merged	87.50	50.00	99.43	73.44	1.62	<u>31.08</u>	<b>72.93</b>	<u>60.44</u>	88.75	72.28
+ LoRA	<u>90.50</u>	<b>69.85</b>	96.55	<b>100.00</b>	0.00	21.04	64.79	29.39	78.81	63.18
+ General Data	87.50	35.20	99.04	73.16	<b>3.49</b>	28.45	70.86	56.93	<b>89.83</b>	<b>74.92</b>
+ OGPSA (Ours)	<u>90.50</u>	63.60	<b>100.00</b>	97.14	<u>3.03</u>	<b>31.31</b>	70.64	<b>63.96</b>	<u>88.98</u>	<u>72.35</u>

Thus, a sufficient condition to preserve reference capability  $i$  to first order is  $\langle g^{(i)}(\theta), \Delta\theta \rangle = 0$ . Enforcing this for all  $i$  yields the linear constraints

$$\langle g^{(i)}(\theta), \Delta\theta \rangle = 0, \quad i = 1, \dots, M, \quad (15)$$

equivalently  $\Delta\theta \in \mathcal{S}_{\text{gen}}(\theta)^\perp$ . Among all feasible directions, the projected gradient achieves the steepest instantaneous decrease of the safety loss.

**Proposition 4.1** (Steepest Feasible Descent). *Let  $f(\theta) = \mathcal{L}_{\text{safe}}(\theta)$  with gradient  $g = \nabla f(\theta)$ , and let  $\mathcal{S}_{\text{gen}}(\theta) = \text{span}\{g^{(i)}(\theta)\}_{i=1}^M$ . Among all unit vectors  $v$  satisfying  $\langle g^{(i)}(\theta), v \rangle = 0$  for all  $i$ , the maximally descending di-*

rection is

$$v^* = -\frac{P_{\mathcal{S}_{\text{gen}}(\theta)^\perp}(g)}{\|P_{\mathcal{S}_{\text{gen}}(\theta)^\perp}(g)\|}. \quad (16)$$

*Proof.* Any feasible  $v$  lies in  $\mathcal{S}_{\text{gen}}(\theta)^\perp$ . Decompose  $g = g_{\parallel} + g_{\perp}$  with  $g_{\parallel} \in \mathcal{S}_{\text{gen}}(\theta)$  and  $g_{\perp} \in \mathcal{S}_{\text{gen}}(\theta)^\perp$ . Then  $\langle g, v \rangle = \langle g_{\perp}, v \rangle$ . By Cauchy–Schwarz (Björck, 1994; Leon et al., 2013), the minimum of  $\langle g_{\perp}, v \rangle$  over  $\|v\| = 1$  is  $-\|g_{\perp}\|$ , achieved when  $v = -g_{\perp}/\|g_{\perp}\|$ .  $\square$

**Algorithm and complexity.** Algorithm 1 summarizes OGPSA. The overhead consists of: (i) an additional  $M$  reference-gradient computations every  $K$  steps (i.e.,  $M$  extra backward passes on small reference mini-batches

per refresh), and (ii) a projection of  $g_{\text{safe}}$  onto a rank- $M'$  subspace, which requires computing  $U_{\tau}^{\top} g_{\text{safe}}$  and forming  $U_{\tau}(U_{\tau}^{\top} g_{\text{safe}})$  (equivalently  $M'$  inner products plus a linear combination). For small  $M'$  and moderate  $K$ , this cost is typically negligible compared to standard backpropagation for safety alignment.

## 5. Experiments

In this section, we describe the experimental setup, then present the results with an in-depth analysis.

### 5.1. Experiments Setup

We evaluate our framework on LLaMA3.1-8B-Instruct (Dubey et al., 2024) and Qwen2.5-7B-Instruct (Yang et al., 2024b) across three standard safety alignment paradigms: SFT, DPO (Rafailov et al., 2023), and sequential SFT-DPO. The safety alignment utilizes a 10k-sample dataset derived from PKU-SafeRLHF (Ji et al., 2024). Apart from the naive tuning method, we compare OGPSA against three established mitigation strategies: (1) *+Merged* (weight interpolation), (2) *+LoRA* (low-rank adaptation), and (3) *+General Data*, a classic replay baseline mixing 10k UltraFeedback (Cui et al., 2024) samples. Further details regarding the experimental setup, including model architectures, datasets, baseline methods, evaluation metrics, and training protocols, are provided in Appendix Sec. A.

### 5.2. Overall Performance

As shown in Table 1 and Fig. 2, standard safety alignment methods (SFT and DPO) impose a heavy alignment tax. This phenomenon is exacerbated in the multi-stage SFT-DPO pipeline, where sequential optimization leads to cumulative forgetting. Specifically, for the Qwen2.5-7B model, *SimpleQA* accuracy collapses from 3.33% (pre-trained) to 0.79% after SFT, and further decays to 0.53% following SFT-DPO. Similarly, instruction-following capabilities (*IFEval*) suffer sequential degradation, dropping from 64.33% to 57.30% (SFT) and finally to 51.94% (SFT-DPO). Existing mitigation strategies fail to fundamentally resolve this conflict. While mixing general data (*+ General Data*) or applying parameter averaging (*+ Merged*) can partially recover general capabilities, they frequently dilute the safety signal. Conversely, while applying parameter regularization (*+ LoRA*) maintains high safety scores, it exacerbates severe forgetting in general abilities (Fig. 2, Table 1).

In contrast, our proposed OGPSA consistently achieves the optimal balance between safety and general utility across most settings. For instance, OGPSA effectively neutralizes the alignment tax: on Qwen2.5-7B Instruct SFT-DPO, it restores *IFEval* scores from 51.94% (naive tuning) back

Table 2. Effect of general capability subspace composition on alignment outcomes using DPO (Rafailov et al., 2023) on Qwen. The best results are marked in **bold**.

Model	Safety ( $\uparrow$ )		Truthful ( $\uparrow$ )		Helpful ( $\uparrow$ )	
	Stereotype	StrongReject	SimpleQA	MMLU	IFEval	HHH
Qwen2.5-7B-Instruct Model	96.74	44.83	3.33	73.50	64.33	88.77
w/o ours	98.47	63.60	1.57	73.43	63.22	87.52
+ w/ 1 dim (Helpful)	98.66	72.75	1.94	73.21	62.48	88.74
+ w/ 1 dim (Truthful)	<b>99.62</b>	70.74	3.17	<b>74.36</b>	61.74	87.54
+ w/ 1 dim (Mixed)	99.23	<b>72.87</b>	3.28	73.07	61.00	89.21
+ w/ 2 dims (Helpful+Truthful)	99.23	72.64	<b>3.35</b>	72.79	<b>63.40</b>	<b>90.68</b>

to 63.96% (approaching the pre-trained 64.33%), and recovers *SimpleQA* scores from 0.53% to 3.03% (vs. 3.33% pre-trained), all while maintaining robust safety compliance. In summary, the robustness of OGPSA is consistent across different models and training stages. As shown in Fig. 2 and Appendix Fig. 4, whether applied to single-stage SFT/DPO or the multi-stage SFT-DPO pipeline, our method consistently establishes a Pareto-superior frontier between safety and general abilities compared to standard baselines.

### 5.3. Ablations

We conduct ablation studies on the Qwen-2.5-7B model (Yang et al., 2024b) to understand the critical components of OGPSA.

**Impact of Subspace Dimensionality and Diversity.** As described by previous study (Aghajanyan et al., 2021; Zhou et al., 2023a), general capabilities can be effectively represented by a few representative dimensions. Based on this, we explore the impact of constructing the projection subspace using reference gradients from single versus diverse domains. As shown in Table 2, our projection method remains effective even when constrained by a single gradient direction. However, the protection is domain-specific: utilizing a reference gradient solely from *UltraFeedback* (Helpful) improve the HHH score (88.74%), but offers limited protection for truthfulness (*SimpleQA* 1.94%). Conversely, using *HaluEval* (Truthful) restores *SimpleQA* to 3.17% but results in lower score in *FEval* and *HHH*. This indicates that while a single reference gradient can mitigate forgetting in its corresponding domain, it may fail to cover the broader spectrum of model capabilities.

Crucially, the results demonstrate the superiority of multi-dimensional constraints. Simply mixing the datasets to compute a single average gradient (“1 dim Mixed”) yields suboptimal results, particularly in instruction following (*IFEval* drops to 61.00%). In contrast, constructing a subspace spanned by two orthogonal directions (“2 dims”)—representing both helpfulness and truthfulness—achieves the best global performance. Results for the SFT setting are reported in Appendix Tab. 6, which exhibit trends consistent with those observed in the DPO experiments. This confirms that orthogonalizing safety updates

Table 3. Robustness of gradient estimation to sample size budgets using DPO (Rafailov et al., 2023) on Qwen. The best results are marked in **bold**.

Model	Safety ( $\uparrow$ )		Truthful ( $\uparrow$ )		Helpful ( $\uparrow$ )	
	Stereotype	StrongReject	SimpleQA	MMLU	IFEval	HHH
Qwen2.5-/B-Instruct Model	96.74	44.83	3.33	73.50	64.33	88.77
w/o ours	98.47	63.60	1.57	<b>73.43</b>	63.22	87.52
+ General Data (10k)	97.32	46.89	3.29	73.21	62.85	87.92
+ w/ 50	99.43	70.69	<b>3.37</b>	72.57	61.18	<b>91.53</b>
+ w/ 100	<b>99.62</b>	71.29	<b>3.37</b>	72.79	<b>64.33</b>	90.68
+ w/ 150	<b>99.62</b>	72.48	3.24	73.00	61.92	90.68
+ w/ 200	99.23	<b>72.64</b>	3.35	72.79	63.40	90.68

Table 4. Effect of subspace update frequency on optimization dynamics using DPO (Rafailov et al., 2023) on Qwen. The best results are marked in **bold**.

Model	Safety ( $\uparrow$ )		Truthful ( $\uparrow$ )		Helpful ( $\uparrow$ )	
	Stereotype	StrongReject	SimpleQA	MMLU	IFEval	HHH
Qwen2.5-7B-Instruct Model	96.74	44.83	3.33	73.50	64.33	88.77
w/o our	98.47	63.60	1.57	73.43	63.22	86.28
+ w/ step 2	<b>99.81</b>	<b>80.59</b>	<b>3.49</b>	72.36	59.89	<b>90.68</b>
+ w/ step 5	99.23	72.64	3.35	72.79	<b>63.40</b>	<b>90.68</b>
+ w/ step 10	97.51	65.04	2.91	72.93	61.92	<b>90.68</b>
+ w/ No updating	98.66	65.07	1.50	<b>74.93</b>	60.81	88.98

against a diverse set of principal components effectively preserves the model’s comprehensive knowledge base without compromising safety alignment.

**Data Efficiency for Gradient Estimation.** To assess the cost-efficiency of our framework, we evaluate how the size of the reference dataset used for gradient estimation effects performance. Employing the 2-dimensional subspace configuration (Helpful + Truthful) established in Table 2, we vary the sample budget for each dimension. As shown in Table 3, OGPSA demonstrates remarkable data efficiency. The DPO stage proves even more robust, achieving optimal stability with as few as 100 samples, recovering *FEval* and *HHH* performance to 64.33% and 90.68%, respectively. In the SFT setting (see Appendix Table 7), increasing the budget to just 200 samples per dimension is sufficient to construct a high-fidelity subspace, surpassing the performance of the *General Data* baseline which relies on mixing 10,000 samples, demonstrating that OGPSA is more data-efficient and effective than brute-force replay. These results indicate that the principal directions of general capabilities are dominant and can be captured with minimal data, making OGPSA a highly efficient alternative to computationally expensive replay strategies.

**Impact of Subspace Update Frequency.** To account for the non-stationarity of the general capability manifold during optimization, we investigate how the frequency of updating the projection subspace affects the alignment trade-off. As shown in Table 4, a dynamic subspace significantly outperforms a static one. Relying on a fixed subspace computed at initialization (“No updating”) leads to stale constraints, causing a severe drop in truthfulness (SimpleQA 1.50%). Conversely, frequent updates capture the local curvature of the parameter space more accurately; specifically, updating every 5 steps yields the optimal trajectory, achieving higher

Table 5. Scalability analysis of OGPSA across model sizes. The best results are marked in **bold**.

Model	Safety ( $\uparrow$ )		Truthful ( $\uparrow$ )		Helpful ( $\uparrow$ )	
	Stereotype	StrongReject	SimpleQA	MMLU	IFEval	HHH
<b>Qwen2.5-0.5B-Instruct</b>						
Instruct Baseline	94.44	38.43	0.69	37.14	22.55	65.75
SFT	79.31	<b>86.53</b>	0.09	36.57	17.19	63.69
SFT + Ours	<b>96.74</b>	85.38	<b>0.88</b>	<b>38.00</b>	<b>23.84</b>	<b>66.29</b>
DPO	65.52	74.75	0.00	<b>36.78</b>	16.08	66.59
DPO + Ours	<b>99.23</b>	<b>79.97</b>	<b>1.06</b>	36.57	<b>22.37</b>	<b>66.69</b>
<b>Qwen2.5-3B-Instruct</b>						
Instruct Baseline	100.00	43.08	1.48	65.36	54.71	80.46
SFT	<b>100.00</b>	<b>69.20</b>	0.37	63.14	51.39	<b>80.45</b>
SFT + Ours	<b>100.00</b>	66.93	<b>1.13</b>	<b>63.93</b>	<b>53.97</b>	78.75
DPO	<b>100.00</b>	59.78	0.37	<b>64.64</b>	52.49	<b>80.04</b>
DPO + Ours	<b>100.00</b>	<b>64.35</b>	<b>1.90</b>	64.50	<b>52.87</b>	79.26
<b>Qwen2.5-7B-Instruct</b>						
Instruct Baseline	96.74	44.83	3.33	73.50	64.33	88.77
SFT	<b>100.00</b>	<b>90.48</b>	0.79	72.00	57.30	<b>88.34</b>
SFT + Ours	<b>100.00</b>	87.43	<b>3.61</b>	<b>73.21</b>	<b>63.03</b>	87.07
DPO	98.47	63.60	1.57	<b>73.43</b>	63.22	87.52
DPO + Ours	<b>99.23</b>	<b>72.64</b>	<b>3.35</b>	72.79	<b>63.40</b>	<b>90.68</b>

safety score than native DPO tuning and recovering *SimpleQA* to 3.35%, *FEval* to 63.40%, *HHH* to 90.68%. In the SFT setting (detailed in Appendix 8), OGPSA requires less frequent updates than DPO, achieving a favorable trade-off with a coarser update frequency of 30 steps. In summary, periodic re-estimation of the reference gradients is essential to ensure the projection remains orthogonal to the evolving general capability subspace.

**Scalability Analysis** To verify the scalability and universality of OGPSA, we evaluate its performance across a spectrum of model scales ranging from 0.5B to 7B parameters. As demonstrated in Table 5, OGPSA consistently mitigates catastrophic forgetting regardless of model capacity or the specific alignment algorithm (SFT or DPO). On the compact Qwen2.5-0.5B, OGPSA restores *SimpleQA* performance from a negligible 0.09% (Standard SFT) to 0.88% while simultaneously boosting *Stereotype* defense by over 17%. This robust trend persists in the 3B and 7B models, where OGPSA consistently recovers general capabilities (e.g., *MMLU* and *FEval*) that are otherwise eroded by standard alignment, without compromising safety compliance. In summary, these results confirm that OGPSA provides a scalable solution to the alignment tax, remaining effective across diverse scales of model parameters.

## 6. Conclusion

In this work, we rigorously characterize the alignment tax as a manifestation of catastrophic forgetting within a heterogeneous continual learning framework. We introduce **Orthogonal Gradient Projection for Safety Alignment (OGPSA)**, a lightweight geometric solution that decouples safety optimization from capability retention by constraining updates to the orthogonal complement of a low-rank general-capability subspace. Extensive empirical validation confirms that OGPSA effectively resolves the stability-

plasticity dilemma, establishing a superior Pareto frontier across diverse models and alignment pipelines. Future avenues for research include investigating high-fidelity subspace construction methods to more comprehensively encapsulate the manifold of general capability, as well as exploring fine-grained, adaptive projection mechanisms to further refine the trade-off between alignment strictness and capability preservation.

## Impact Statement

This paper presents work whose goal is to advance the field of Machine Learning. There are many potential societal consequences of our work, none which we feel must be specifically highlighted here.

## References

Achiam, J., Adler, S., Agarwal, S., Ahmad, L., Akkaya, I., Aleman, F. L., Almeida, D., Altenschmidt, J., Altman, S., Anadkat, S., et al. Gpt-4 technical report. *arXiv preprint arXiv:2303.08774*, 2023.

Aghajanyan, A., Gupta, S., and Zettlemoyer, L. Intrinsic dimensionality explains the effectiveness of language model fine-tuning. In *Proceedings of the 59th annual meeting of the association for computational linguistics and the 11th international joint conference on natural language processing (volume 1: long papers)*, pp. 7319–7328, 2021.

Askell, A., Bai, Y., Chen, A., Drain, D., Ganguli, D., Henighan, T., Jones, A., Joseph, N., Mann, B., DasSarma, N., et al. A general language assistant as a laboratory for alignment. *arXiv preprint arXiv:2112.00861*, 2021.

Bai, J., Bai, S., Chu, Y., Cui, Z., Dang, K., Deng, X., Fan, Y., Ge, W., Han, Y., Huang, F., et al. Qwen technical report. *arXiv preprint arXiv:2309.16609*, 2023.

Bianchi, F., Suzgun, M., Attanasio, G., Rottger, P., Jurafsky, D., Hashimoto, T., and Zou, J. Safety-tuned llamas: Lessons from improving the safety of large language models that follow instructions. In *The Twelfth International Conference on Learning Representations*, 2024.

Björck, Å. Numerics of gram-schmidt orthogonalization. *Linear Algebra and Its Applications*, 197:297–316, 1994.

Buzzega, P., Boschini, M., Porrello, A., Abati, D., and Calderara, S. Dark experience for general continual learning: a strong, simple baseline. *Advances in neural information processing systems*, 33:15920–15930, 2020.

Chao, P., Robey, A., Dobriban, E., Hassani, H., Pappas, G. J., and Wong, E. Jailbreaking black box large language models in twenty queries. In *2025 IEEE Conference on Secure and Trustworthy Machine Learning (SaTML)*, pp. 23–42. IEEE, 2025.

Chen, M., Tworek, J., Jun, H., Yuan, Q., Pinto, H. P. D. O., Kaplan, J., Edwards, H., Burda, Y., Joseph, N., Brockman, G., et al. Evaluating large language models trained on code. *arXiv preprint arXiv:2107.03374*, 2021.

Choi, H. K., Du, X., and Li, Y. Safety-aware fine-tuning of large language models. In *Neurips Safe Generative AI Workshop 2024*, 2024.

Cobbe, K., Kosaraju, V., Bavarian, M., Chen, M., Jun, H., Kaiser, L., Plappert, M., Tworek, J., Hilton, J., Nakano, R., et al. Training verifiers to solve math word problems. *arXiv preprint arXiv:2110.14168*, 2021.

Cui, G., Yuan, L., Ding, N., Yao, G., He, B., Zhu, W., Ni, Y., Xie, G., Xie, R., Lin, Y., et al. Ultrafeedback: Boosting language models with scaled ai feedback. In *Proceedings of the 41st International Conference on Machine Learning*, volume 235, pp. 9722–9744, 2024.

Dai, J., Pan, X., Sun, R., Ji, J., Xu, X., Liu, M., Wang, Y., and Yang, Y. Safe rlhf: Safe reinforcement learning from human feedback. In *The Twelfth International Conference on Learning Representations*, 2024.

Dong, Y., Chen, H., Chen, J., Fang, Z., Yang, X., Zhang, Y., Tian, Y., Su, H., and Zhu, J. How robust is google’s bard to adversarial image attacks? *arXiv preprint arXiv:2309.11751*, 2023.

Dubey, A., Jauhri, A., Pandey, A., Kadian, A., Al-Dahle, A., Letman, A., Mathur, A., Schelten, A., Yang, A., Fan, A., et al. The llama 3 herd of models. *arXiv preprint arXiv:2407.21783*, 2024.

Farn, H., Su, H., Kumar, S. H., Sahay, S., Chen, S.-T., and Lee, H.-y. Safeguard fine-tuned llms through pre-and post-tuning model merging. *arXiv preprint arXiv:2412.19512*, 2024.

Guan, M. Y., Joglekar, M., Wallace, E., Jain, S., Barak, B., Heylar, A., Dias, R., Vallone, A., Ren, H., Wei, J., et al. Deliberative alignment: Reasoning enables safer language models. *arXiv preprint arXiv:2412.16339*, 2024.

Hendrycks, D., Burns, C., Basart, S., Zou, A., Mazeika, M., Song, D., and Steinhardt, J. Measuring massive multitask language understanding. In *International Conference on Learning Representations*, 2021a.

Hendrycks, D., Burns, C., Kadavath, S., Arora, A., Basart, S., Tang, E., Song, D., and Steinhardt, J. Measuring mathematical problem solving with the math dataset. In *Proceedings of the Neural Information Processing Systems Track on Datasets and Benchmarks*, volume 1, 2021b.

Hu, E. J., Shen, Y., Wallis, P., Allen-Zhu, Z., Li, Y., Wang, S., Wang, L., Chen, W., et al. Lora: Low-rank adaptation of large language models. *ICLR*, 1(2):3, 2022.

Huang, Y., Zhang, Y., Chen, J., Wang, X., and Yang, D. Continual learning for text classification with information disentanglement based regularization. In *Proceedings of the 2021 Conference of the North American Chapter of the Association for Computational Linguistics: Human Language Technologies*, pp. 2736–2746, 2021.

Inan, H., Upasani, K., Chi, J., Rungta, R., Iyer, K., Mao, Y., Tontchev, M., Hu, Q., Fuller, B., Testuggine, D., et al. Llama guard: Llm-based input-output safeguard for human-ai conversations. *arXiv preprint arXiv:2312.06674*, 2023.

Jaech, A., Kalai, A., Lerer, A., Richardson, A., El-Kishky, A., Low, A., Helyar, A., Madry, A., Beutel, A., Carney, A., et al. Openai o1 system card. *arXiv preprint arXiv:2412.16720*, 2024.

Ji, J., Hong, D., Zhang, B., Chen, B., Dai, J., Zheng, B., Qiu, T., Li, B., and Yang, Y. Pku-saferlhf: A safety alignment preference dataset for llama family models. *arXiv preprint arXiv:2406.15513*, 2024.

Kantharaj, S., Do, X. L., Leong, R. T., Tan, J. Q., Hoque, E., and Joty, S. Opencqa: Open-ended question answering with charts. In *Proceedings of the 2022 Conference on Empirical Methods in Natural Language Processing*, pp. 11817–11837, 2022.

Kirk, R., Mediratta, I., Nalmpantis, C., Luketina, J., Hambro, E., Grefenstette, E., and Raileanu, R. Understanding the effects of rlhf on llm generalisation and diversity. In *The Twelfth International Conference on Learning Representations*, 2024.

Kirkpatrick, J., Pascanu, R., Rabinowitz, N., Veness, J., Desjardins, G., Rusu, A. A., Milan, K., Quan, J., Ramalho, T., Grabska-Barwinska, A., et al. Overcoming catastrophic forgetting in neural networks. *Proceedings of the national academy of sciences*, 114(13):3521–3526, 2017.

Kowsher, M., Prottasha, N. J., and Bhat, P. Propulsion: Steering llm with tiny fine-tuning. In *Proceedings of the 31st International Conference on Computational Linguistics*, pp. 7569–7597, 2025.

Lee, S., Seong, H., Lee, D. B., Kang, M., Chen, X., Wagner, D., Bengio, Y., Lee, J., and Hwang, S. J. Harmaug: Effective data augmentation for knowledge distillation of safety guard models. In *The Thirteenth International Conference on Learning Representations*, 2025.

Leon, S. J., Björck, Å., and Gander, W. Gram-schmidt orthogonalization: 100 years and more. *Numerical Linear Algebra with Applications*, 20(3):492–532, 2013.

Li, J., Cheng, X., Zhao, X., Nie, J.-Y., and Wen, J.-R. Haluval: A large-scale hallucination evaluation benchmark for large language models. In *The 2023 Conference on Empirical Methods in Natural Language Processing*.

Li, Z. and Hoiem, D. Learning without forgetting. *IEEE transactions on pattern analysis and machine intelligence*, 40(12):2935–2947, 2017.

Lin, S., Yang, L., Fan, D., and Zhang, J. Trgp: Trust region gradient projection for continual learning. In *The Tenth International Conference on Learning Representations*, 2022.

Lin, Y., Lin, H., Xiong, W., Diao, S., Liu, J., Zhang, J., Pan, R., Wang, H., Hu, W., Zhang, H., Dong, H., Pi, R., Zhao, H., Jiang, N., Ji, H., Yao, Y., and Zhang, T. Mitigating the alignment tax of RLHF. In *Proceedings of the 2024 Conference on Empirical Methods in Natural Language Processing*, pp. 580–606, 2024.

Liu, G., Zhu, Y., Chen, J., and Jiang, M. Scientific algorithm discovery by augmenting alphaevolve with deep research. *arXiv preprint arXiv:2510.06056*, 2025.

Liu, Y., Deng, G., Xu, Z., Li, Y., Zheng, Y., Zhang, Y., Zhao, L., Zhang, T., Wang, K., and Liu, Y. Jailbreaking chatgpt via prompt engineering: An empirical study. *arXiv preprint arXiv:2305.13860*, 2023.

Lopez-Paz, D. and Ranzato, M. Gradient episodic memory for continual learning. *Advances in neural information processing systems*, 30, 2017.

Lu, Y., Zhang, S., Cheng, D., Xing, Y., Wang, N., Wang, P., and Zhang, Y. Visual prompt tuning in null space for continual learning. *Advances in neural information processing systems*, 37:7878–7901, 2024.

McDonnell, M. D., Gong, D., Parvaneh, A., Abbasnejad, E., and van den Hengel, A. Ranpac: Random projections and pre-trained models for continual learning. *NeurIPS*, 36, 2024.

Nam, D., Macvean, A., Hellendoorn, V., Vasilescu, B., and Myers, B. Using an llm to help with code understanding. In *Proceedings of the IEEE/ACM 46th International Conference on Software Engineering*, pp. 1–13, 2024.

Noukhovitch, M., Lavoie, S., Strub, F., and Courville, A. C. Language model alignment with elastic reset. *Advances in Neural Information Processing Systems*, 36:3439–3461, 2023.

Ouyang, L., Wu, J., Jiang, X., Almeida, D., Wainwright, C., Mishkin, P., Zhang, C., Agarwal, S., Slama, K., Ray, A., et al. Training language models to follow instructions with human feedback. *Advances in neural information processing systems*, 35:27730–27744, 2022.

Papineni, K., Roukos, S., Ward, T., and Zhu, W.-J. Bleu: a method for automatic evaluation of machine translation. In *Proceedings of the 40th annual meeting of the Association for Computational Linguistics*, pp. 311–318, 2002.

Qiao, J., Zhang, Z., Tan, X., Qu, Y., Zhang, W., Han, Z., and Xie, Y. Gradient projection for continual parameter-efficient tuning. *IEEE Transactions on Pattern Analysis and Machine Intelligence*, 2025.

Rafailov, R., Sharma, A., Mitchell, E., Manning, C. D., Ermon, S., and Finn, C. Direct preference optimization: Your language model is secretly a reward model. *Advances in neural information processing systems*, 36: 53728–53741, 2023.

Rebedea, T., Derczynski, L., Ghosh, S., Sreedhar, M. N., Brahman, F., Jiang, L., Li, B., Tsvetkov, Y., Parisien, C., and Choi, Y. Guardrails and security for llms: Safe, secure and controllable steering of llm applications. In *Proceedings of the 63rd Annual Meeting of the Association for Computational Linguistics (Volume 5: Tutorial Abstracts)*, pp. 13–15, 2025.

Rein, D., Hou, B. L., Stickland, A. C., Petty, J., Pang, R. Y., Dirani, J., Michael, J., and Bowman, S. R. Gpqa: A graduate-level google-proof q&a benchmark. In *First Conference on Language Modeling*, 2024.

Röttger, P., Kirk, H., Vidgen, B., Attanasio, G., Bianchi, F., and Hovy, D. XSTest: A test suite for identifying exaggerated safety behaviours in large language models. In *Proceedings of the 2024 Conference of the North American Chapter of the Association for Computational Linguistics: Human Language Technologies (Volume 1: Long Papers)*, pp. 5377–5400, 2024.

Souly, A., Lu, Q., Bowen, D., Trinh, T., Hsieh, E., Pandey, S., Abbeel, P., Svegliato, J., Emmons, S., Watkins, O., and Toyer, S. A strongreject for empty jailbreaks. In *Advances in Neural Information Processing Systems*, volume 37, pp. 125416–125440, 2024.

Sudhakaran, S., González-Duque, M., Freiberger, M., Glanois, C., Najarro, E., and Risi, S. Mariopt: Open-ended text2level generation through large language models. *Advances in Neural Information Processing Systems*, 36:54213–54227, 2023.

Wang, B., Xu, C., Wang, S., Gan, Z., Cheng, Y., Gao, J., Awadallah, A. H., and Li, B. Adversarial glue: A multi-task benchmark for robustness evaluation of language models. In *Proceedings of the Neural Information Processing Systems Track on Datasets and Benchmarks*, volume 1, 2021.

Wang, B., Chen, W., Pei, H., Xie, C., Kang, M., Zhang, C., Xu, C., Xiong, Z., Dutta, R., Schaeffer, R., Truong, S., Arora, S., Mazeika, M., Hendrycks, D., Lin, Z., Cheng, Y., Koyejo, S., Song, D., and Li, B. Decodingtrust: A comprehensive assessment of trustworthiness in gpt models. In *Advances in Neural Information Processing Systems*, volume 36, pp. 31232–31339, 2023.

Wang, L., Zhang, X., Su, H., and Zhu, J. A comprehensive survey of continual learning: Theory, method and application. *IEEE transactions on pattern analysis and machine intelligence*, 46(8):5362–5383, 2024a.

Wang, Y., Li, H., Han, X., Nakov, P., and Baldwin, T. Do-not-answer: Evaluating safeguards in LLMs. In *Findings of the Association for Computational Linguistics: EACL 2024*, pp. 896–911, 2024b.

Wang, Z., Zhang, Z., Lee, C.-Y., Zhang, H., Sun, R., Ren, X., Su, G., Perot, V., Dy, J., and Pfister, T. Learning to prompt for continual learning. In *CVPR*, pp. 139–149, 2022.

Wang, Z., Bi, B., Pentyala, S. K., Ramnath, K., Chaudhuri, S., Mehrotra, S., Mao, X.-B., Asur, S., et al. A comprehensive survey of llm alignment techniques: Rlhf, rlaif, ppo, dpo and more. *arXiv preprint arXiv:2407.16216*, 2024c.

Wang, Z., Yang, F., Wang, L., Zhao, P., Wang, H., Chen, L., Lin, Q., and Wong, K.-F. SELF-GUARD: Empower the LLM to safeguard itself. In Duh, K., Gomez, H., and Bethard, S. (eds.), *Proceedings of the 2024 Conference of the North American Chapter of the Association for Computational Linguistics: Human Language Technologies (Volume 1: Long Papers)*, pp. 1648–1668, Mexico City, Mexico, June 2024d. Association for Computational Linguistics. doi: 10.18653/v1/2024.naacl-long.92. URL <https://aclanthology.org/2024.naacl-long.92/>.

Wei, J., Karina, N., Chung, H. W., Jiao, Y. J., Papay, S., Glaese, A., Schulman, J., and Fedus, W. Measuring short-form factuality in large language models. *arXiv preprint arXiv:2411.04368*, 2024.

Wortsman, M., Ilharco, G., Kim, J. W., Li, M., Kornblith, S., Roelofs, R., Lopes, R. G., Hajishirzi, H., Farhadi, A., Namkoong, H., et al. Robust fine-tuning of zero-shot models. In *Proceedings of the IEEE/CVF conference on computer vision and pattern recognition*, pp. 7959–7971, 2022.

Wu, L., Wang, M., Xu, Z., Cao, T., Oo, N., Hooi, B., and Deng, S. Automating steering for safe multimodal large language models. In *Proceedings of the 2025 Conference on Empirical Methods in Natural Language Processing*, pp. 792–814, 2025a.

Wu, Y., Piao, H., Huang, L.-K., Wang, R., Li, W., Pfister, H., Meng, D., Ma, K., and Wei, Y. Sd-lora: Scalable decoupled low-rank adaptation for class incremental learning. In *ICLR*, 2025b.

Yang, E., Wang, Z., Shen, L., Liu, S., Guo, G., Wang, X., and Tao, D. Adamerging: Adaptive model merging for multi-task learning. In *The Twelfth International Conference on Learning Representations*, 2024a.

Yang, Q. A., Yang, B., Zhang, B., Hui, B., Zheng, B., Yu, B., Li, C., Liu, D., Huang, F., Dong, G., Wei, H., Lin, H., Yang, J., Tu, J., Zhang, J., Yang, J., Yang, J., Zhou, J., Lin, J., Dang, K., Lu, K., Bao, K., Yang, K., Yu, L., Li, M., Xue, M., Zhang, P., Zhu, Q., Men, R., Lin, R., Li, T., Xia, T., Ren, X., Ren, X., Fan, Y., Su, Y., Zhang, Y.-C., Wan, Y., Liu, Y., Cui, Z., Zhang, Z., Qiu, Z., Quan, S., and Wang, Z. Qwen2.5 technical report. *ArXiv*, abs/2412.15115, 2024b. URL <https://api.semanticscholar.org/CorpusID:274859421>.

Zeng, Y., Lin, H., Zhang, J., Yang, D., Jia, R., and Shi, W. How johnny can persuade LLMs to jailbreak them: Rethinking persuasion to challenge AI safety by humanizing LLMs. In *Proceedings of the 62nd Annual Meeting of the Association for Computational Linguistics (Volume 1: Long Papers)*, pp. 14322–14350, 2024.

Zhang, G., Wang, L., Kang, G., Chen, L., and Wei, Y. Slca: Slow learner with classifier alignment for continual learning on a pre-trained model. *arXiv preprint arXiv:2303.05118*, 2023.

Zhang, Y., Zhang, S., Huang, Y., Xia, Z., Fang, Z., Yang, X., Duan, R., Yan, D., Dong, Y., and Zhu, J. Stair: Improving safety alignment with introspective reasoning. In *Forty-second International Conference on Machine Learning*, 2025.

Zhao, W., Ren, X., Hessel, J., Cardie, C., Choi, Y., and Deng, Y. Wildchat: 1m chatgpt interaction logs in the wild. In *The Twelfth International Conference on Learning Representations*, 2024.

Zheng, Y., Zhang, R., Zhang, J., YeYanhan, Y., and Luo, Z. Llamafactory: Unified efficient fine-tuning of 100+ language models. In *Proceedings of the 62nd Annual Meeting of the Association for Computational Linguistics (Volume 3: System Demonstrations)*, pp. 400–410, 2024.

Zhou, C., Liu, P., Xu, P., Iyer, S., Sun, J., Mao, Y., Ma, X., Efrat, A., Yu, P., Yu, L., et al. Lima: Less is more for alignment. *Advances in Neural Information Processing Systems*, 36:55006–55021, 2023a.

Zhou, D.-W., Sun, H.-L., Ning, J., Ye, H.-J., and Zhan, D.-C. Continual learning with pre-trained models: a survey. In *Proceedings of the Thirty-Third International Joint Conference on Artificial Intelligence*, pp. 8363–8371, 2024a.

Zhou, J., Lu, T., Mishra, S., Brahma, S., Basu, S., Luan, Y., Zhou, D., and Hou, L. Instruction-following evaluation for large language models. *arXiv preprint arXiv:2311.07911*, 2023b.

Zhou, Z., Liu, J., Shao, J., Yue, X., Yang, C., Ouyang, W., and Qiao, Y. Beyond one-preference-fits-all alignment: Multi-objective direct preference optimization. In *Findings of the Association for Computational Linguistics: ACL 2024*, pp. 10586–10613, 2024b.

## A. Detailed Experimental Setups

In this work, we conduct all our experiments on clusters with 8 NVIDIA A800 GPUs.

**Models and Datasets.** We conduct experiments using two widely adopted instruction-tuned Large Language Models: LLaMA3.1-8B-Instruct (Dubey et al., 2024) and Qwen2.5-7B-Instruct (Yang et al., 2024b). For the safety alignment phase, we utilize a seed dataset  $\mathcal{D}_{\text{safe}}$  consisting of 10k samples sampled from PKU-SafeRLHF (Ji et al., 2024), where the SFT labels and DPO chosen labels are refuse response generated by gpt-4o-mini, and DPO rejected labels are select from the most unsafe answer from the original dataset. To simulate the standard practice of data replay for maintaining general capabilities, we draw 10k pairwise samples from UltraFeedback (Cui et al., 2024) as the general data source. Where the SFT labels and DPO chosen labels are selected from the highest score answer from original dataset, and DPO rejected labels are select from the lowest score answer. For our proposed method (OGPSA), we require a small reference set to estimate the general capability subspace. To efficiently capture the essential dimensions of general utility (Aghajanyan et al., 2021; Zhou et al., 2023a), we sample a minimal budget of data to represent key competencies: (1) *Helpfulness*: 200 samples randomly selected from UltraFeedback (Cui et al., 2024). (2) *Truthfulness*: 200 samples randomly selected from HaluEval (Li et al.), where the SFT labels and DPO chosen labels are correct answers, and DPO rejected labels are hallucinated answers. We preprocess the hallucinated answers to be the same format of the correct answers to prevent reward hacking on the answer format. This highlights the data efficiency of our approach compared to replay-based methods.

**Baselines.** We evaluate our framework against three standard safety alignment paradigms: Supervised Fine-Tuning (SFT), Direct Preference Optimization (DPO) (Rafailov et al., 2023), and Sequential SFT-DPO. To benchmark the mitigation of the Alignment Tax, we compare OGPSA against three representative regularization and replay strategies applied to the standard paradigms: (1) *+Merged*: A weight-interpolation method that linearly averages the parameters of the pre-trained model and the safety-aligned model to balance capabilities (Farn et al., 2024; Wortsman et al., 2022). (2) *+LoRA*: parameter-efficient fine-tuning using low-rank adaptation, which acts as a regularization constraint by updating only a small subset of parameters (Hu et al., 2022). (3) *+General Data*: A classic experience replay approach that mixes the 10k general samples from UltraFeedback (Cui et al., 2024) into the safety training data.

**Training Details** We have done all the training of LLMs with LLaMA-Factory (Zheng et al., 2024), which is a popular toolbox for LLM training. Consistent with established protocols (Zhang et al., 2025), all models are trained for 3 epochs during the SFT stage and 1 epoch during the DPO stage. We tune the learning rate  $1e - 6$  and  $\beta$  for DPO from 0.2. Batch size is fixed as 128 and weight decay is set to 0. We adopt a cosine scheduler with a warm-up ratio of 0.1. Following the official implementation, we set learning rate  $1e - 4$  for LoRA. For the subspace update frequency  $K$ . We set  $K = 30$  for all SFT and  $K = 5$  for DPO experiments.

**Evaluation.** We employ a comprehensive suite of 10 benchmarks to evaluate the trade-off between safety and general utility. *Safety (Harmlessness)*: Following established protocols (Guan et al., 2024), models are evaluated on their ability to refuse harmful queries. We utilize StrongReject (Souly et al., 2024), XSTest (Röttger et al., 2024), the toxic split of WildChat (Zhao et al., 2024), and the stereotype split of Do-Not-Answer (Wang et al., 2024b). For StrongReject, we report the average defense success score against the top-2 jailbreak attacks (PAIR (Chao et al., 2025) and PAP (Zeng et al., 2024)), while reporting refusal rates for other datasets. *General Utility*: We assess diverse capabilities including truthfulness via SimpleQA (Wei et al., 2024), GPQA (Rein et al., 2024), and MMLU (Hendrycks et al., 2021a), and general helpfulness via BIG-bench HHH (Zhou et al., 2024b) and instruction following via IFEval (Zhou et al., 2023b). Additionally, we evaluate adversarial robustness using AdvGLUE (Wang et al., 2021). We report the official metrics for all benchmarks. For evaluation, we use default temperature for generation to guarantee the reproducibility by default. Below, we introduce the benchmarks and corresponding metrics in detail.

For StrongReject (Souly et al., 2024), we take the official evaluation protocol, which uses GPT-4o-mini to evaluate the responses and gives a rubric-based score reflecting the willingness and capabilities in responding to harmful queries. We follow (Jaech et al., 2024) and take the goodness score, which is  $1 - \text{rubric score}$ , as the metric. We evaluate models on prompts with no jailbreak in addition to the reported top-2 jailbreak methods PAIR (Chao et al., 2025), and PAP-Misrepresentation (Zeng et al., 2024). For main results, we only report the average goodness score on the two jailbreak methods, since most methods achieve goodness scores near 1.0. For XsTest (Röttger et al., 2024), we select the unsafe split to evaluate the resistance to normal harmful queries and follow its official implementation on refusal determination with GPT-4o-mini. We report the sum of full refusal rate and partial refusal rate as the metric. For WildChat (Zhao et al., 2024), we

filter the conversations with ModerationAPI<sup>1</sup> and eventually get 219 samples with high toxicity in English. For Stereotype, it is a split for evaluating the model's refusal behavior to queries associated with fairness issues in Do-Not-Answer (Wang et al., 2024b).

## B. Theoretical Derivations

In this section, we provide the general mathematical foundation for Proposition 1 presented in the main text. We prove that for any differentiable function, the direction of steepest descent restricted to a linear subspace is equivalent to the negative gradient projected onto that subspace.

### B.1. Steepest Descent Direction in a Linear Subspace

**Formalization.** Let  $V = \mathbb{R}^d$  be a  $d$ -dimensional Euclidean space (representing the parameter space of the LLM) equipped with the standard inner product  $\langle \cdot, \cdot \rangle$  and the induced norm  $\|\cdot\|$ . Consider the following definitions:

- Let  $f : \mathbb{R}^d \rightarrow \mathbb{R}$  be a differentiable scalar function (representing the loss function  $\mathcal{L}$ ).
- Let  $g = \nabla f(\theta) \in \mathbb{R}^d$  denote the gradient of  $f$  at point  $\theta$ .
- Let  $\mathcal{S} \subseteq \mathbb{R}^d$  be a linear subspace of  $V$  (representing the allowable optimization subspace, e.g.,  $\mathcal{S}_{\text{gen}}^\perp$ ).
- Let  $P_{\mathcal{S}} : \mathbb{R}^d \rightarrow \mathcal{S}$  denote the orthogonal projection operator onto  $\mathcal{S}$ .

**Objective:** We seek a unit vector  $v \in \mathcal{S}$  (i.e.,  $\|v\| = 1$ ) that maximizes the rate of descent, equivalent to minimizing the directional derivative  $D_v f(\theta)$ .

**Lemma B.1** (Optimal Descent in Subspace). *Assume  $P_{\mathcal{S}}(g) \neq 0$ . The direction  $v^* \in \mathcal{S}$  that minimizes the directional derivative of  $f$  is given by:*

$$v^* = -\frac{P_{\mathcal{S}}(g)}{\|P_{\mathcal{S}}(g)\|}. \quad (17)$$

*In other words, the steepest descent direction within a subspace is the negative of the orthogonally projected gradient.*

*Proof.* **Step 1: Definition of the Directional Derivative.** The directional derivative of  $f$  at  $\theta$  along  $v$  is given by:

$$D_v f(\theta) = \langle \nabla f(\theta), v \rangle = \langle g, v \rangle. \quad (18)$$

**Step 2: Orthogonal Decomposition.** By the Projection Theorem, the gradient  $g$  can be uniquely decomposed into a component within  $\mathcal{S}$  and a component orthogonal to  $\mathcal{S}$ :

$$g = g_{\mathcal{S}} + g_{\perp}, \quad (19)$$

where  $g_{\mathcal{S}} = P_{\mathcal{S}}(g) \in \mathcal{S}$  and  $g_{\perp} \in \mathcal{S}^\perp$ . By definition, for any vector  $u \in \mathcal{S}$ , the inner product  $\langle g_{\perp}, u \rangle = 0$ .

**Step 3: Simplifying the Objective.** We minimize  $\langle g, v \rangle$  subject to  $v \in \mathcal{S}$  and  $\|v\| = 1$ . Substituting the decomposition:

$$\langle g, v \rangle = \langle g_{\mathcal{S}} + g_{\perp}, v \rangle = \langle g_{\mathcal{S}}, v \rangle + \underbrace{\langle g_{\perp}, v \rangle}_{0} = \langle g_{\mathcal{S}}, v \rangle. \quad (20)$$

**Step 4: Minimization via Cauchy-Schwarz.** The problem reduces to minimizing the inner product  $\langle g_{\mathcal{S}}, v \rangle$  subject to unit norm. By the Cauchy-Schwarz (Björck, 1994; Leon et al., 2013) inequality:

$$|\langle g_{\mathcal{S}}, v \rangle| \leq \|g_{\mathcal{S}}\| \|v\| = \|g_{\mathcal{S}}\|. \quad (21)$$

This implies:

$$-\|g_{\mathcal{S}}\| \leq \langle g_{\mathcal{S}}, v \rangle \leq \|g_{\mathcal{S}}\|. \quad (22)$$

<sup>1</sup><https://platform.openai.com/docs/guides/moderation>

The lower bound (maximum descent) is achieved if and only if  $v$  is collinear to  $g_S$  and points in the opposite direction. Thus, the optimal vector is:

$$v^* = -\frac{g_S}{\|g_S\|} = -\frac{P_S(g)}{\|P_S(g)\|}. \quad (23)$$

□

**Connection to Main Text:** In the context of OGPSA, the subspace  $S$  corresponds to the null space of general capabilities  $S_{\text{gen}}^\perp$ , and the function  $f$  corresponds to the safety loss  $\mathcal{L}_{\text{safe}}$ . This lemma proves that our update rule follows the optimal path for safety optimization constrained within the non-forgetting zone.

## C. Appendix Results

### C.1. Overall Performance of Llama

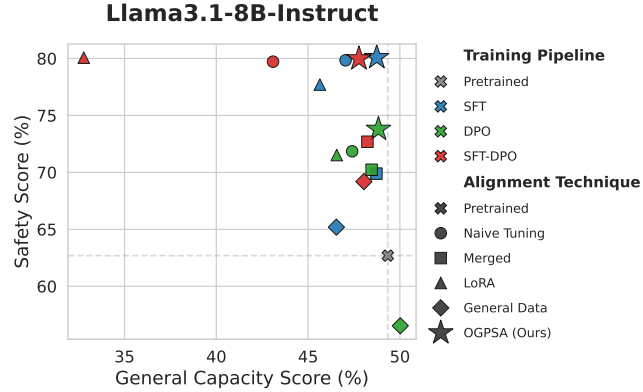


Figure 4. Overall performance of alignment strategies on Llama3.1-8B-Instruct. We report the aggregate *Safety Score* (avg. of 4 datasets) and *General Capacity Score* (avg. of 6 datasets); see Table 1 for details.

### C.2. Impact of Subspace Dimensionality and Diversity using SFT

Table 6. Effect of general capability subspace composition on alignment outcomes using SFT on Qwen. We investigate how the diversity of reference data (Helpfulness vs. Truthfulness) and the dimensionality of the constraint subspace (1 vs. 2 directions) impact the alignment outcomes. The best results are marked in **bold**.

Model	Safety ( $\uparrow$ )		Truthful ( $\uparrow$ )		Helpful ( $\uparrow$ )	
	Stereotype	StrongReject	SimpleQA	MMLU	IFEval	HHH
Qwen2.5-7B-Instruct Model	96.74	44.83	3.33	73.50	64.33	88.77
w/o ours	<b>100.00</b>	90.48	0.79	72.00	57.30	88.34
+ 1 dim (Helpfulness)	<b>100.00</b>	<b>91.60</b>	1.16	<b>73.36</b>	58.04	87.50
+ 1 dim (Truthfulness)	<b>100.00</b>	86.09	<b>3.70</b>	73.14	62.85	87.92
+ 1 dim (Mixed)	99.81	88.60	3.49	72.50	<b>63.40</b>	<b>88.74</b>
+ 2 dim (Helpfulness+Truthfulness)	<b>100.00</b>	87.43	3.61	73.21	63.03	87.07

### C.3. Impact of Sample Size Budgets for Gradient Estimation

**Table 7. Robustness of gradient estimation to sample size budgets using DPO (Rafailov et al., 2023) on Qwen.** We evaluate the performance stability as the number of samples used to estimate the reference capability gradients increases. Our method remains effective even with limited data budgets. The **best** results are marked in **bold**.

Model	Safety ( $\uparrow$ )		Truthful ( $\uparrow$ )		Helpful ( $\uparrow$ )	
	Stereotype	StrongReject	SimpleQA	MMLU	IFEval	HHH
Qwen2.5-7B-Instruct Model	96.74	44.83	3.33	73.50	64.33	88.77
w/o ours	<b>100.00</b>	<b>90.48</b>	0.79	72.00	57.30	88.34
+ General Data (10k)	99.04	70.38	3.47	69.93	53.42	86.28
+ w/ 50	<b>100.00</b>	86.87	3.35	71.71	61.74	89.16
+ w/ 100	<b>100.00</b>	85.61	3.54	72.43	63.22	88.73
+ w/ 150	<b>100.00</b>	87.37	3.47	<b>73.21</b>	<b>63.03</b>	<b>89.97</b>
+ w/ 200	<b>100.00</b>	87.43	<b>3.61</b>	<b>73.21</b>	<b>63.03</b>	87.07

### C.4. Impact of Subspace Update Frequency using SFT

**Table 8. Effect of subspace update frequency on optimization dynamics using SFT on Qwen.** We compare static subspaces against dynamic updates at varying intervals. The **best** results are marked in **bold**.

Model	Safety ( $\uparrow$ )		Truthful ( $\uparrow$ )		Helpful ( $\uparrow$ )	
	Stereotype	StrongReject	SimpleQA	MMLU	IFEval	HHH
Qwen2.5-7B-Instruct Model	96.74	44.83	3.33	73.50	64.33	88.77
w/o ours	<b>100.00</b>	<b>90.48</b>	0.79	72.00	57.30	88.34
+ w/ step 5	<b>100.00</b>	89.76	<b>3.68</b>	71.36	61.92	88.27
+ w/ step 15	<b>100.00</b>	87.69	3.56	72.29	<b>64.14</b>	88.34
+ w/ step 30	<b>100.00</b>	87.43	3.61	73.21	63.03	87.07
+ w/ No updating	<b>100.00</b>	89.04	1.02	<b>73.29</b>	58.04	<b>89.57</b>